ELSEVIER

Nanomedicine: Nanotechnology, Biology, and Medicine
xx (xxxx) xxx

nanomedicine
Nanotechnology, Biology, and Medicine

nanomedjournal.com

Graphical Abstract

Nanomedicine: Nanotechnology, Biology, and Medicine xxx (2019) xxx–xxx

Iguratimod encapsulated PLGA-NPs improves therapeutic outcome in glioma, glioma stem-like cells and temozolomide resistant glioma cells

Muhammad Younis[a], Wang Faming[b], Zhao Hongyan[b], Tan Mengmeng[b], Song Hang[a], Yuan Liudi[a,b,*]

[a]*Key Laboratory for Developmental Genes and Human Disease, Ministry of Education, Institute of Life Sciences, Southeast University, Nanjing, China*
[b]*Department of Biochemistry and Molecular Biology, Medical School of Southeast University, Nanjing, China*

Figure 1. **Graphical scheme of this study.** We investigated the anti-cancer effect of Iguratimod Encapsulated PLGA-NPs (IGU-PLGA-NPs) using *in vitro* and *in vivo* models of glioma, glioma like stem cells and TMZ-resistant glioma. Our results showed that IGU-PLGA-NPs inhibited proliferation and migration, improved apoptosis and cell cycle arrest and were specifically delivered to targeted site inside the brain.

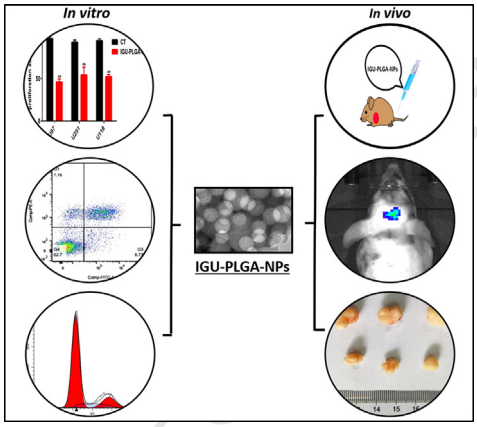

ELSEVIER
Nanomedicine: Nanotechnology, Biology, and Medicine
xx (xxxx) xxx
nanomedicine Nanotechnology, Biology, and Medicine
nanomedjournal.com

Iguratimod encapsulated PLGA-NPs improves therapeutic outcome in glioma, glioma stem-like cells and temozolomide resistant glioma cells

Q4 Q3 Muhammad Younis[a], Wang Faming[b], Zhao Hongyan[b], Tan Mengmeng[b], Song Hang[a], Yuan Liudi[a,b,*]

[a]*Key Laboratory for Developmental Genes and Human Disease, Ministry of Education, Institute of Life Sciences, Southeast University, Nanjing, China*
[b]*Department of Biochemistry and Molecular Biology, Medical School of Southeast University, Nanjing, China*

Revised 17 September 2019

Abstract

Glioma is the most common neoplasm of the central nervous system, with the highest mortality rate. The present study was designed to examine the therapeutic effect of Iguratimod (IGU) encapsulated-poly (lactic-co-glycolic acid) PLGA nanoparticles (IGU-PLGA-NPs), which showed inhibition of glioma cells proliferation both *in vitro* and *in vivo*. IGU encapsulated in PLGA nanoparticles with an average size of 100-200 nm was prepared using modified double-emulsion (W1/O/W2) method. Cell Counting Kit-8 (CCK-8) analysis of Glioma cancer cells and glioma stem-like cells (GSCs) demonstrated significant inhibition of their growth treated with IGU-PLGA-NPs. IGU-PLGA-NPs inhibit migration in glioma cells as well as tumor sphere formation in GSCs. Treatment with IGU-PLGA-NPs showed a significant decrease in tumor growth through the apoptotic pathway in mice model without any visible organ toxicity and it can successfully cross the blood brain barrier (BBB). Most Importantly, IGU-PLGA-NPs significantly depleted growth of U251 Temozolomide-resistant (U251TMZ-R) cells.

Key words: Cancer; Glioma; Apoptosis; PLGA; Iguratimod

Glioma is one of the most common malignant cancers derived from glial cells in the central nervous system with poor prognosis.[1] Several therapeutic strategies including surgery, radiotherapy, and chemotherapy have been developed for the treatment of glioma but no obvious improvements have been obtained.[2] Uncontrolled and rapid cell proliferation of glioma grows aggressively resulting in severe recurrence, and because of insensitivity to chemotherapy, patients usually have a poor prognosis.[3,4] The failure of existing strategies for the treatment of glioma has been attributed to the presence of a subpopulation of cancer cells known as glioma stem-like cells (GSCs), which have the ability to resist chemo-radiotherapeutics because of their unique characteristics.[5] Therefore, more complex treatments capable of overcoming the ability of GSCs to eliminate anticancer drugs and with other protective functions are urgently needed.

Additionally, effective delivery is the major obstacle for the development of any chemotherapy against glioblastoma because BBB prevents delivery of therapeutic molecules and blood born chemicals to the brain. Blood brain barrier only allows small, lipid soluble and electrically neutral drugs to the brain. Various approaches have been discovered for achieving higher drug concentrations in the brain of glioma patients, such as chemically modified drugs and prodrugs, temporary disruption of the BBB[6], intra-arterial delivery[7], and receptor-mediated delivery.[8] Therefore, there is a persistent need to develop advanced approach for more potent and effective treatment for brain tumor, that might ideally distribute and provide localized higher concentrations of drugs in the malignant tissue across the BBB without causing any systemic toxicity.

In this context, nanomaterials could play an important role because of their unique properties that are found neither in bulk materials nor in single molecules and which are necessary to develop advanced cancer treatments.[9,10] Poly (lactic-co-glycolic acid) (PLGA) NPs have several benefits, like the biocompatible,

Q1 **Statement:** There are no commercial associations, current and within the past five years, that might pose a potential, perceived or real conflict of interest.

Conflict of Interest: The authors declare no competing financial interests.

Funding: This work was supported by the open funds of the Key Laboratory for Developmental Genes and Human Disease, Ministry of Q2 Education, China (201801).

*Corresponding author at: Key Laboratory for Developmental Genes and Human Disease, Ministry of Education, Institute of Life Sciences, Southeast University, Nanjing, China.
E-mail address: yld@seu.edu.cn. (

https://doi.org/10.1016/j.nano.2019.102101
1549-9634/© 2019 Published by Elsevier Inc.

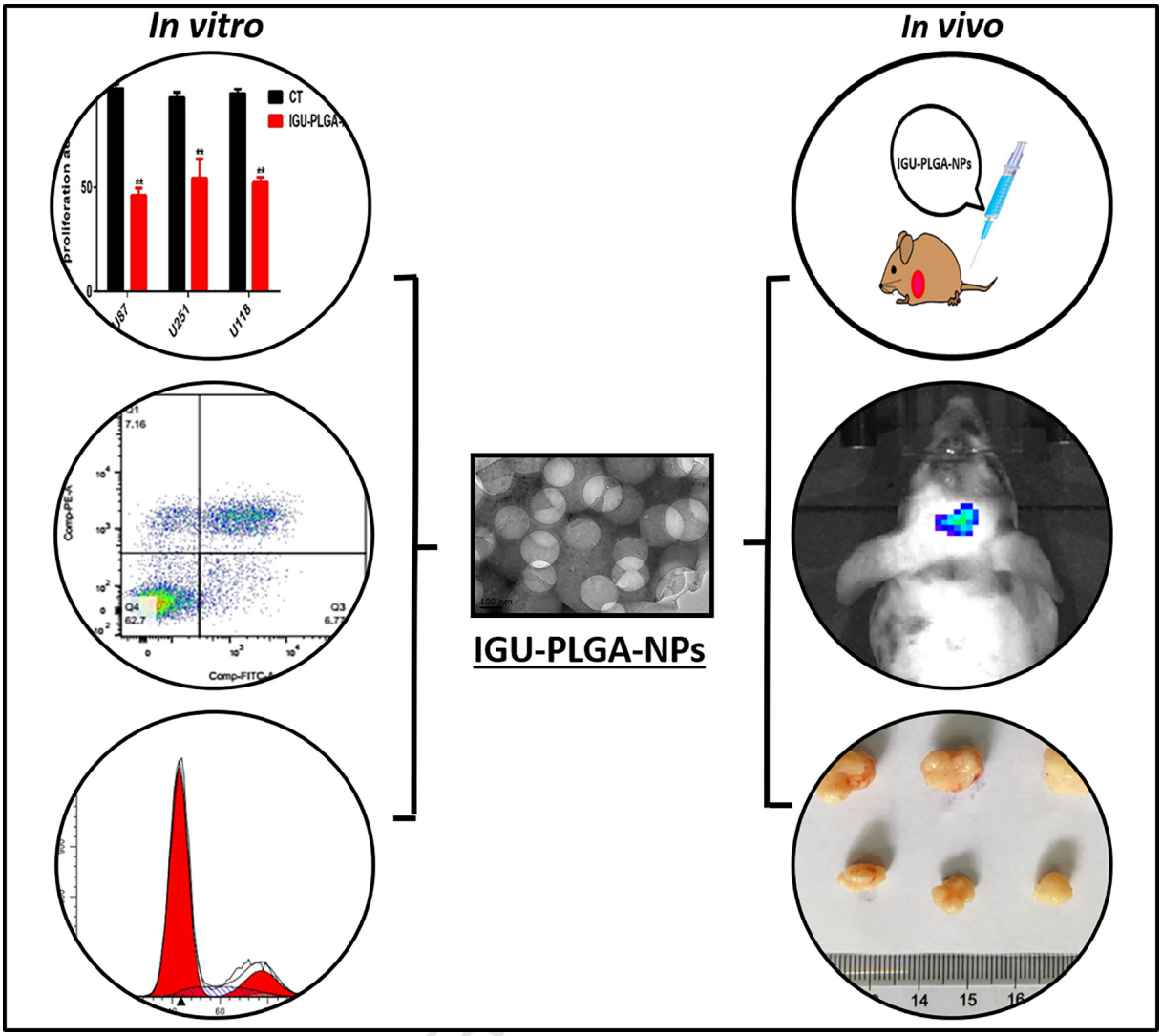

Figure 1. **Graphical scheme of the study.** We investigated the anti-cancer effect of IGU-PLGA-NPs using *in vitro* and *in vivo* models of glioma, GSCs and TMZ-resistant glioma. Our results showed that IGU-PLGA-NPs inhibits proliferation, migration, improve apoptosis, cell cycle arrest and specifically delivered to targeted site inside the brain.

biodegradable, sustained release of encapsulated drugs after intracellular endocytosis, and being inexpensive and approved by Food and Drug Administration (FDA).[11] Iguratimod (IGU) is a novel anti-inflammatory and anti-rheumatic drug for the treatment of rheumatoid arthritis that prevents generation of immunoglobins and inflammatory cytokines such as tumor necrosis factor alpha (TNF-α) and Interleukins (IL-1β-IL-6, IL-8, IL-17). IGU also inhibits IL-8 in hepatocellular carcinogenesis.[12,13]

In this study, to achieve a higher concentration of drug in the brain of glioma patients we have prepared IGU encapsulated PLGA NPs (IGU-PLGA-NPs); due to their too small size, NPs can cross the biological barriers easily, without blocking circulation of blood. For the first time, we have analyzed the anti-cancer effect of Iguratimod encapsulated PLGA nanoparticles (IGU-PLGA NPs) *in vitro* and *in vivo* and it did not lead to any vital organ toxicity in glioma (Figure 1). Complete blood cells (CBC) analysis did not show significant change after IGU-PLGA-NPs treatment in mice model. We have found out that IGU-PLGA-NPs inhibit proliferation and migration as well as improve apoptosis and cell cycle arrest in glioma. IGU-PLGA-NPs depleted the growth, tumor sphere formation as well as CD133 expression of GSCs. Interestingly, IGU-PLGA-NPs can cross BBB and it has an antiproliferative effect against TMZ-resistant glioma cells. The interesting results highlight, for the very first time, the therapeutic potentiality of IGU-PLGA-NPs to decreased tumor growth of brain cancer.

Methods

Cell culture

Human Glioma cells (U87, U118, and U251) were obtained from the cell Bank of type culture collection of Chinese

Academy of Sciences (Shanghai, China). U251 Temozolomide (TMZ)-resistant cells were a generous gift from Dr. Fawad Ur Rehman, Henan University, Kaifeng, China. All cell lines were grown in DMEM (Hyclone) with 10% FBS (Gibco) in a cell culture incubator with 5% CO_2 at 37 °C. The glioma stem-like cells were isolated by using serum free clone formation method.[14,15] Serum free medium was comprised of DMEM/F12 medium (Hyclone), 20 mg/mL of B27 (Invitrogen), 20 ng/mL of basic fibroblast growth factor (Sigma), 20 ng/mL of EGF (PeproTech). After 8-10 days of culture, primary tumor sphere was detected and subsequently dissociated and passaged in 72-96 h in fresh medium.

Preparation of PLGA-Nanoparticles encapsulated with Iguratimod

PLGA-NPs were fabricated using a double-emulsion water-in-oil-in-water method with slight modifications.[16] Briefly, 100 mg of PLGA (Daigang Co, Jinan, China) was dissolved in 5 mL of dichloromethane; then 200 μL of an aqueous solution containing 30μg/mL of IGU (Simcere, China) as an internal water phase was added. The emulsion was formed by sonicating the mixture by a probe sonicator (Microson XL 2000, Misonix Inc., Farmingdale, NY) for the 30 s at 20 kHz and 30% amplitude. The primary emulsion was quickly mixed in 5 mL of 4% PVA (polyvinyl alcohol solution; Sigma Aldrich) (external water phase) and homogenized for 30 min at 6000 rpm. Then, 5 mL of deionized water was added and the solution was stirred overnight at room temperature to evaporate the dichloromethane. PVA was removed from NPs by washing three times with double distilled water and then activated using EDC (1-ethyl-3-(3 dimethylaminopropyl) carbodiimide hydrochloride), NHS (N-hydroxy-succinimide; Sigma), and PEI (polyethyleneimine; Sigma) also added dropwise to the solution with magnetic stirring and incubated for 2 h at 20 °C. Finally, PEI conjugated NPs were washed twice with deionized water and stored at 4 °C for further use.

Characterization of PLGA-NPs and IGU-PLGA-NPs

The morphology of the PLGA and IGU-PLGA-NPs was characterized by using Transmission electron microscopy (TEM, JEOL JEM-2100). The size distribution and zeta potential were measured by using the PALS Zeta instrument (Brookenhaven instrument Corporation).

CCK-8 assay

The cell numbers were determined by a CCK-8 assay. Glioma cells were cultured into 96-well plates at a density of 1×10^4 cells per well. Optical density (OD) at 450 nm was estimated by the Microplate Reader (Bio-Rad, USA). In addition, GSCs and TMZ-resistant cells viability also determined by CCK-8 assay.

Wound healing assay

Migration of cells was examined by wound healing migration assay as previously reported with modifications.[17] Glioma cells were seeded 3×10^5 well plates for 24 h. Cells were treated with IGU-PLGA-NPs, IGU and control wells; only DMEM was added. *In vitro* scratch wound was made by scraping the cell layer with a tip of the 10 μl pipette. After wounding, suspended cells were washed and fresh medium was added and visualized with an inverted microscope to assess cell migration ability.

Migration assay

Cell migration was determined by Transwell (24-well, 8 μm pore size; Corning) as per reported method.[18] Briefly, 600 μL culture medium was added in the lower chamber, whereas 2×10^5 cells (U87, U118, U251) suspended in 200 μL medium (serum free) were loaded in the upper chamber. Cells on the lower surface of the chamber were stained with 0.1% crystal violate (Sigma) for 20 min. Five randomly selected fields were imaged for cell counting by using a microscope (Olympus, Japan).

Trypan blue assay

To assess the cell viability of U87, U118, and U251, trypan blue assay was performed. Cells were trypsinized and collected in the pellet. Cells were resuspended in PBS and an equal amount of Trypan blue (Sigma) was added. Cell viability was calculated as the percentage of living cells divided by a total number of cells.

Tumor sphere formation assay

Glioma-stem cells (GSCs) were dissociated to single cells and cultured at a density of 200 cells/well in 24-well plates in three groups (Control, IGU, and IGU-PLGA-NPs). The number and diameter of tumor sphere were calculated after 7 days.

Detection of Apoptosis and cell cycle

Apoptosis of U87 and U251 cells were analyzed after 24 h in Control, IGU and IGU-PLGA-NPs treated groups. In apoptosis assay, cells were stained with Propidium Iodide (PI) and Annexin V-FITC (Vazyme, China) and detected by flow cytometry. For cell cycle detection, cells (1×10^5) were treated at 37 °C and 5% CO_2 for 24 h. The cells were trypsinized and collected by centrifugation (2000 rpm, 5 min) and resuspended in 70% ethanol for 24 h at 4 °C. Afterward, cells were analyzed by flow cytometer.

Protein expression detection using western blotting

Western blot analysis was performed as a standard procedure previously described.[19] Briefly, the following antibodies were used: CD133 (1:1000), Bax (1:2000), Bcl2 (1:1000), Caspase-3 (1:500), Caspase-9 (1:200), CyclinD1 (1:2000), Survivin (1:500) and Glyceraldehyde 3-phosphate dehydrogenase (GAPDH) (1:3000). GAPDH was used as the loading control. After 24 h treatment of cultured cells, protein expression was quantified by western blotting. RIPA lysis buffer was used as a lysis buffer and protein concentration was detected by BCA kit. Then 100 μg protein was loaded in 10% acrylamide gel before transferring to PVDF membrane which was blocked by 5% milk for 1 h. Membrane was probed in primary antibody for 12 h at 4 °C and then in secondary

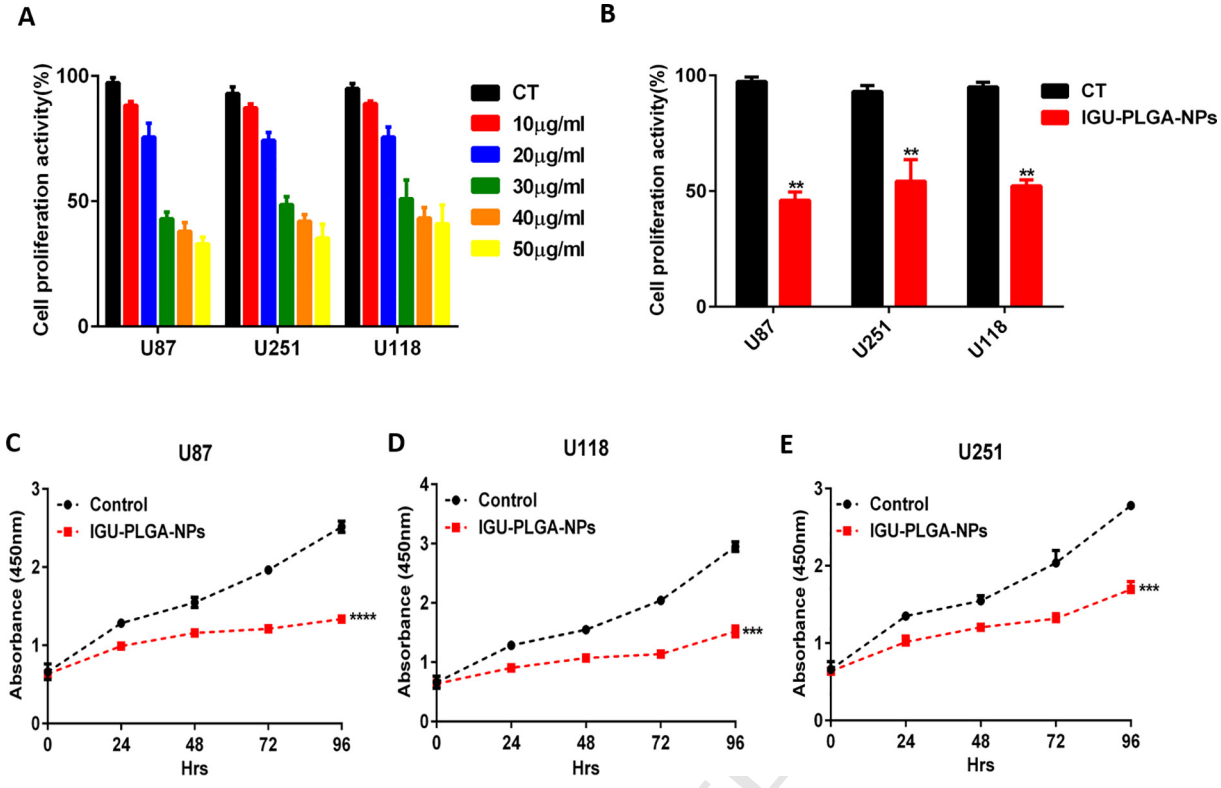

Figure 2. **IGU-PLGA-NPs suppress glioma cell growth.** The proliferation of glioma cells was analyzed by CCK-8 assay after treated by different concentration of IGU (**A**) and IGU-PLGA-NPs (**B**). IGU-PLGA-NPs significantly inhibited the proliferation of glioma cells after treatment compared to the control group (**C-E**) (**$P < 0.01$, ***$P < 0.001$ and ****$P < 0.0001$).

antibody for 1-2 h at room temperature. Proteins expressions were determined by chemiluminescence.

Animal studies

The xenograft tumor mice model was generated by subcutaneous injection of U87 glioma cells (5×10^6 cells) in 0.2 ml media without serum. The cells were implanted into the lateral thoracic region of BALB/c athymic nude mice (male, aged 3-4 weeks and 18-20 g weight) supplied by the KeyGENBioTECH corp., Ltd. After 4 weeks, the xenograft tumor mice model was generated. Mice were injected with IGU-PLGA-NPs (*via* the tail vein), whereas the control group was injected with placebo (PBS). After 18 days, mice were euthanized by cervical dislocation, and the vital organs were harvested for further analysis. All animals' experiments were performed under the guidelines of the National Institute of Health [20] and the Animal Care Research Advisory committee of Southeast University. The animals were regularly monitored for discomfort or pain.

In Vivo BBB FL bioimaging by ICG-IGU-PLGA-NPs

For the *in vivo* fluorescence imaging of nanoparticles in the brain, ICG-IGU-PLGA-NPs were prepared by previously reported method.[21] Then, mice were anesthetized by 5% isoflurane mix with oxygen. Mice were injected (*via* the tail vein) with ICG-IGU-PLGA-NPs, whereas the control group was injected with PBS. *In vivo* bioimaging was performed after 24 h of injection by using the IVIS Lumina FL imaging system.[22] The FL was analyzed by the PerkinElmer software.

Histopathology

For histopathological analysis, vital organs (Heart, liver, kidney, lungs, spleen, and tumor) were fixed in 10% formalin solution for 24 h and processed, prior to the paraffin embedding technique. Tissue sections of vital organs were stained with hematoxylin and eosin (H&E) staining. The histopathology samples were observed in under microscope (ABX53, Olympus, Japan).

Blood sampling and blood CP analysis

The intracardiac injection was used to collect blood under isoflurane anesthesia. Blood was transferred into an EDTA (ethylenediaminetetraacetic acid) tube for complete blood cell (CBC) count analysis (XE-2100 Sysmex).

Statistical analysis

GraphPad Prism 6 software (GraphPad Software, Inc., USA) was used for all performed test. Data were analyzed using the One-way analysis of variance (ANOVA, for multiple samples) or two-tailed Student t test (for two samples). All data are shown as the mean ± S.D. $P < 0.05$ was considered statistically significant.

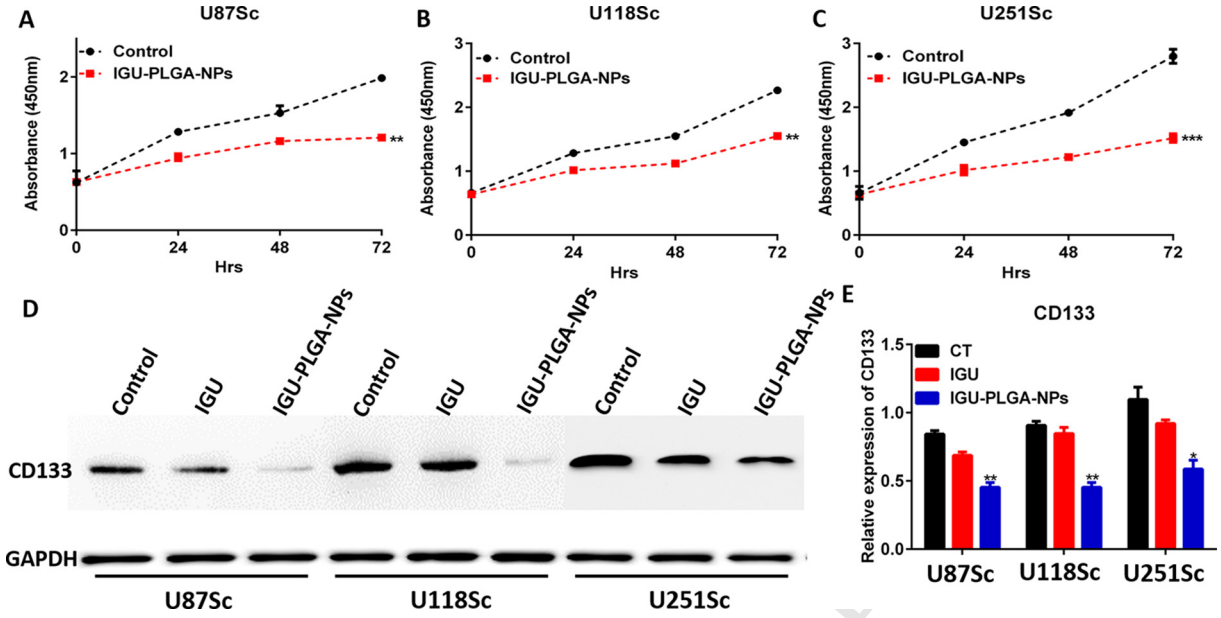

Figure 3. **GSCs growth inhibited by IGU-PLGA-NPs.** The result of the CCK-8 assay indicated that GSCs growth was inhibited by IGU-PLGA-NPs treatment (**A**-**C**). Stem cell marker CD133 expression level was also reduced in treated groups compared to control (**D**, **E**) (*$P < 0.05$, **$P < 0.01$ ***$P < 0.001$).

Results

Characterization of IGU-PLGA-NPs

The average diameters of empty PLGA NPs and IGU-PLGA-NPs were 148 ± 2.5 nm and 199.6 nm, respectively (Figure S1, *A*, *B*). Zeta potential analysis of PLGA NPs revealed negative charges −2.61 Mv (Figure S1, *C*) and zeta potential of IGU-PLGA-NPs was −1.68 Mv (Figure S1, *D*). TEM images showed a spherical shape and smooth external surface, with an averaged diameter, ranging from 100 to 200 nm (Figure S1, *E*, *F*).

IGU-PLGA-NPs inhibited glioma cell proliferation

To study the effect of IGU-PLGA-NPs on the growth of glioma cells (U87, U118, and U251), we detected the influence of IGU and IGU-PLGA-NPs on glioma cells using CCK-8 assay. The cells were treated with alone IGU at different concentration and IGU-PLGA-NPs (Figure 2, *A*, *B*). After 4 days of treatment, significant inhibition of cell proliferation by IGU-PLGA-NPs was detected as compared to control (Figure 2, *C*-*E*). Moreover, we also assessed the cytotoxic effect of IGU-PLGA-NPs on the growth of glioma cancer cell lines using a trypan blue assay after 48 h treatment. Glioma cells showed much lower viability when treated with IGU-PLGA-NPs compared to IGU and control (Figure S2, *A*-*C*).

IGU-PLGA-NPs inhibit cell migration

Cell migration of U87 and U118 was detected by wound healing assay, which revealed suppression of wound closure up to 48 h after IGU-PLGA-NPs treatment, when the gap was partly filled with glioma cells in IGU treated and control group (Figure S3). In addition, we also determined the abilities of cell migration which was a significant aspect of cancer progression. As shown in Figure S4, U87, U118 and U251 glioma cell migration was significantly inhibited in IGU-PLGA-NPs treated group compared with IGU treated and control group in a Transwell assay (Figure S4).

IGU-PLGA-NPs inhibited GSCs proliferation and stemness

CCK-8 assay of GSCs revealed that the cell proliferation of GSCs was significantly reduced in IGU-PLGA-NPs treated groups compared to control groups (Figure 3, *A*-*C*). Additionally, cancer stem-like cells marker CD133 expression was also reduced after IGU-PLGA-NPs treated in GSCs as compared to IGU treated group (Figure 3, *D*, *E*).

Self-renewal ability of GSCs decreased after IGU-PLGA-NPs treatment

To investigate the effect of IGU-PLGA-NPs on GSCs, we analyzed the tumor sphere formation ability of GSCs. As compared to IGU and control, tumor sphere displayed a significantly decreased diameter after IGU-PLGA-NPs treated group. The above results revealed that IGU-PLGA-NPs could decrease the stemness of GSCs as a tumor growth suppressor (Figure 4, *A*-*D*).

IGU-PLGA-NPs induces apoptosis

We examined whether apoptosis is involved in the effect of IGU-PLGA-NPs on glioma cells. The proportion of apoptotic cells was determined by staining of cells with PI and Annexin V-FITC using flow cytometry. A sizable increase of apoptosis induced by IGU-PLGA-NPs was observed compared with the control (Figure 5, *A*-*D*). The mechanism of IGU-PLGA-NPs induced apoptosis was evaluated by analyzing the mitochondrial apoptosis proteins

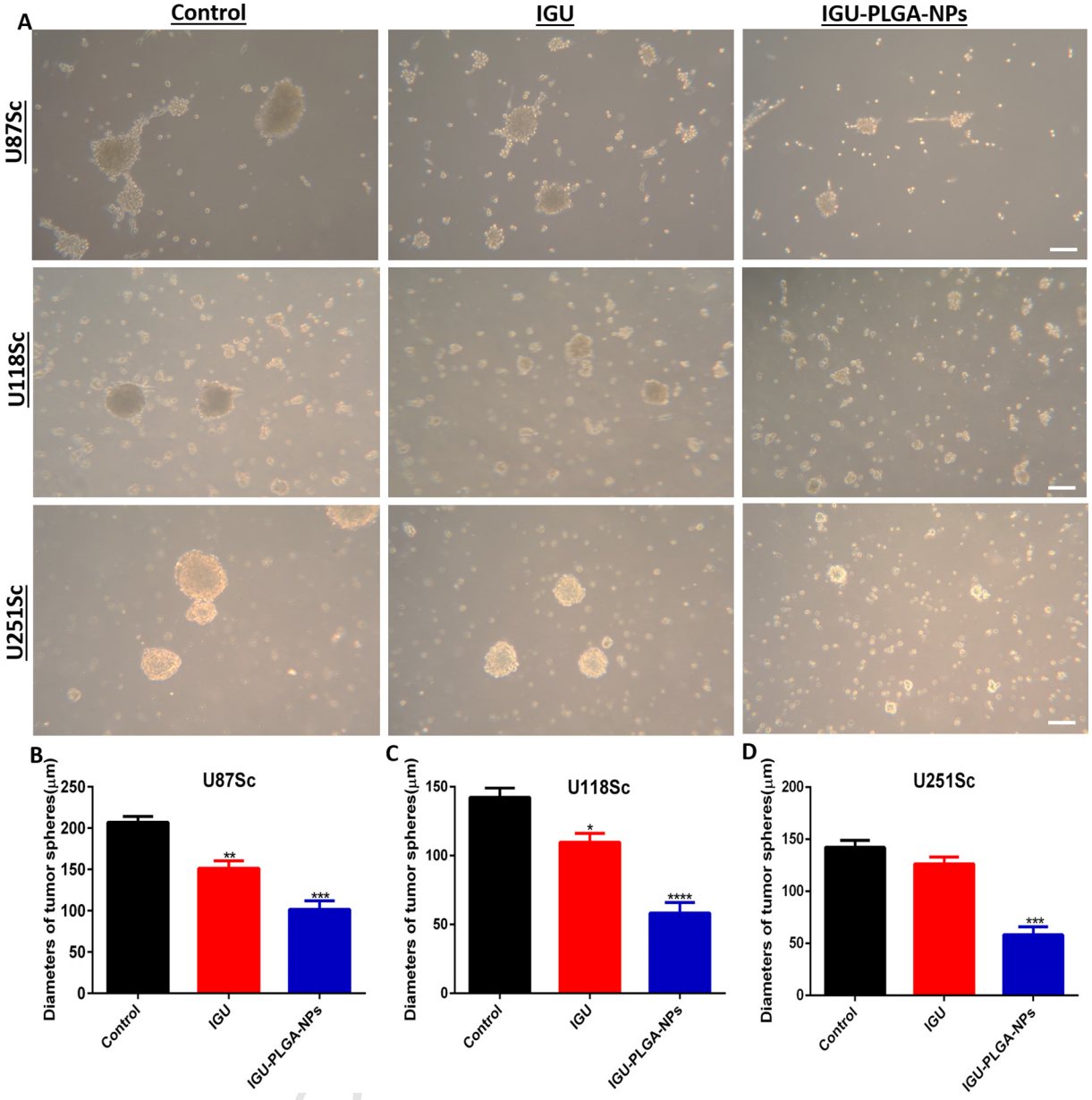

Figure 4. **IGU-PLGA-NPs inhibited Glioma tumor sphere formation.** GSCS were cultured IGU-PLGA-NPs and without IGU-PLGA-NPs as a control for 7 days. Tumor sphere diameter was decreased in treated groups (**A**). The graph indicates the differences in tumor sphere diameter (**B-D**). Scale bar, 200 μm (***$P < 0.001$ and ****$P < 0.0001$).

expression level through western blotting. As shown in Figure S5, compared with the control group, glioma cells exposed to IGU-PLGA-NPs displayed a reduction of anti-apoptotic protein Bcl-2 expression level, and pro-apoptotic protein Bax expression was increased. In addition, the Caspase-3 and Caspase-9 protein expression was increased following the treatment with IGU-PLGA-NPs (Figure S5).

IGU-PLGA-NPs induced G1 phase cell cycle arrest

The impact of IGU and IGU-PLGA-NPs on cell cycle distribution was analyzed by using flow cytometry. IGU-PLGA-NPs significantly increased the cell numbers at G1 phase (60%) after 48 h of treatment as compared to control and IGU (Figure 6, *A-D*). To explore the underlying mechanism of the growth inhibitory effect of IGU-PLGA-NPs, cell cycle regulators critical to the G1 phase checkpoint were assessed, including cyclinD1 and survivin. Western blot analysis confirmed that IGU-PLGA-NPs downregulated the protein expression levels in cyclinD1 and survivin compared with the control group (Figure S6).

IGU-PLGA-NPs suppresses tumor growth in vivo and crosses BBB

BALB/c athymic nude mice were used to observe whether IGU-PLGA-NPs may induce similar effects *in vivo*.

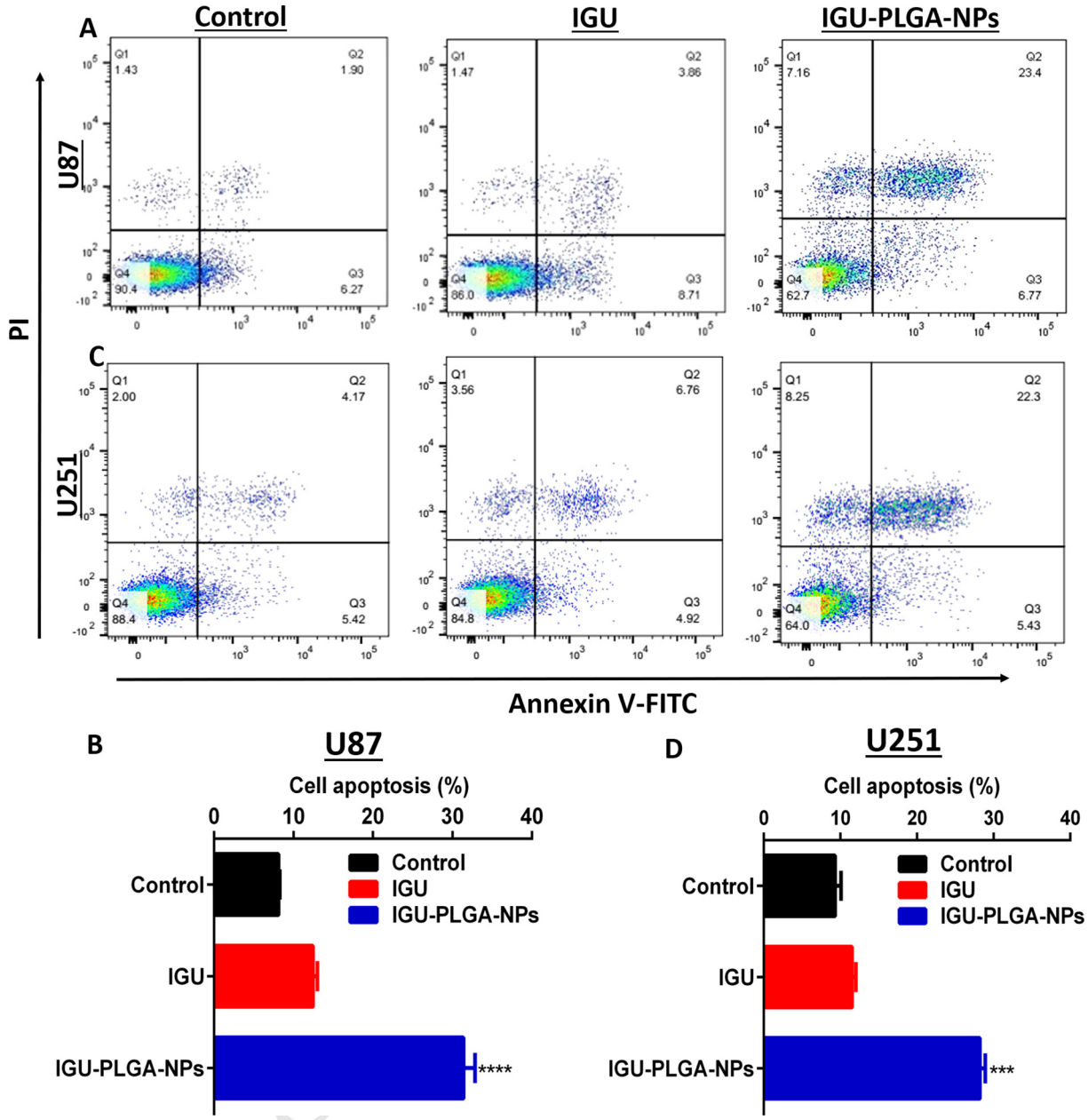

Figure 5. **Apoptosis induced after IGU-PLGA-NPs treatment.** Cells were treated by IGU-PLGA-NPs, IGU for 48 h, stained with PI and Annexin V-FITC, and analyzed by flow cytometry (**A**, **C**). Apoptosis ratio was calculated as the Q2 plus Q4 areas. The percentage of the apoptotic cell population was represented in the graph (**B**, **D**). (***$P < 0.001$ and ****$P < 0.0001$).

Macroscopically, xenograft treated with IGU-PLGA-NPs grew at a significantly slower rate compared with that treated with PBS (Figure 7, *A*). No considerable difference was observed in the weight of mice during all measured days in treated and the control group (Figure 7, *B*). Notably, the tumor growth curve in IGU-PLGA-NPs treated mice had a relatively slow trend compared with the control group (Figure 7, *C*, *E*). H&E staining showed a greater number of dead cells evident in the apoptotic proportion in IGU-PLGA-NPs treated tumor tissue compared with control. Histopathological analysis of heart, liver, kidney, lungs and spleen tissues from control and treated mice showed no apparent lesion formation in organs after treatment in all mice (Figure 7, *F*). Additionally, the fluorescence (FL) signal of ICG-IGU-PLGA-NPs was exclusively found in the brain region of BALB/c athymic mice after 24 h injection while in the control group no fluorescence was noticed (Figure 7, *D*). In addition, IGU-PLGA-NPs had no significant effect on red blood cells, white blood cells, platelets and hemoglobin in treated groups. The treatment had no significant effect of neutrophils, lymphocytes, monocytes, basophiles, and eosinophils (Figure S7).

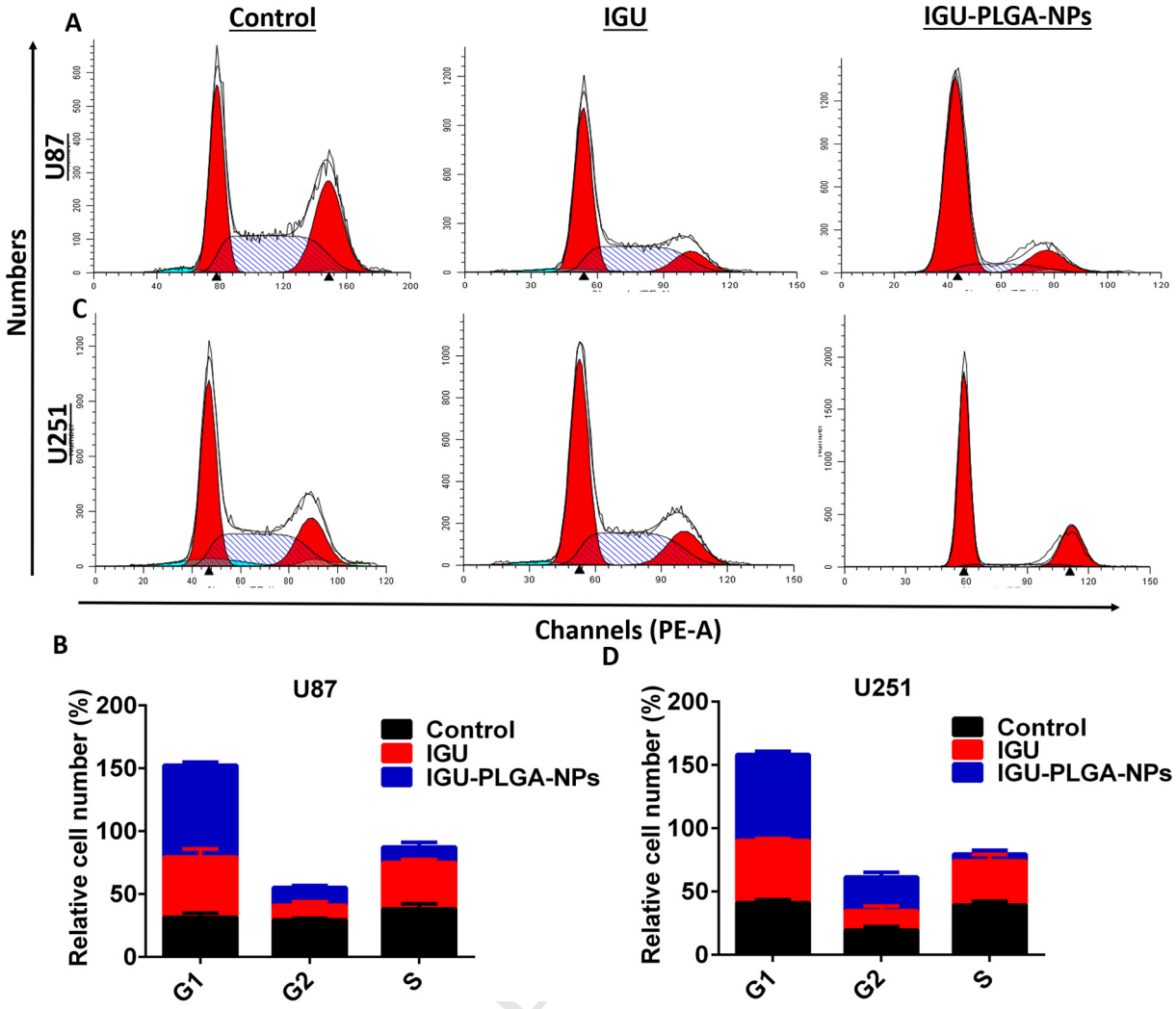

Figure 6. **Effect of IGU-PLGA-NPs on cell cycle arrest.** Glioma cells were treated by IGU-PLGA-NPs and IGU for 48 h. Representative histograms showed the changes in the cell cycle of U87 and U251 (**A**, **C**). Graph represents the percentage of cell cycle distribution (**B**, **D**).

U251TMZ-resistant cells growth significantly reduced by IGU-PLGA-NPs

To find out the effect of IGU-PLGA-NPs on the growth of TMZ-resistant glioma cells line (U251TMZ-R), we detected the impact of IGU and IGU-PLGA-NPs on resistant glioma cells using CCK-8 kit method. The cells were treated with IGU-PLGA-NPs (Figure S8). After 96 h of treatment, significant inhibition of cell growth by IGU-PLGA-NPs was detected in U251TMZ-resistant cells.

Discussion

Malignant glioma cannot be completely cured by surgical resection due to its infiltrative nature and is the main reason of death. Temozolomide (TMZ) treatment was safe and effective but travels slowly in blood flow into the interior of glioma, and has difficulty crossing the BBB. Chemotherapeutic therapy of glioma can provide high local drug concentration, reduce toxicities and improve patient drug compliance.[23–25] Therefore, there is a crucial need for the development of more effective, safe and better therapeutic option against TMZ-sensitive and TMZ-resistant glioma cells. PLGA is a well-known biodegradable polymer and has a long history of safe pharmacological and therapeutic applications.[26,27] PLGA nanoparticles have provided the efficient delivery systems for chemotherapeutics due to their low cytotoxicity, which is the critical parameter for medicinal use.[28]

Different pathways of cancerous cells can be targeted for therapy in which the apoptotic pathways have been considered more promising to inhibit the growth of tumor.[29] Apoptosis is a process of cellular self-destruction and it plays an important role in homeostasis. Apoptotic cells exhibit several biochemical and morphological changes in cells such as apoptotic body formation, cell shrinkage, loss of cell to cell connections, caspase activation, DNA condensation, and fragmentation. Our results indicated that IGU-PLGA-NPs induced apoptosis in glioma cells *in vitro* and *in vivo*. In the current study we have

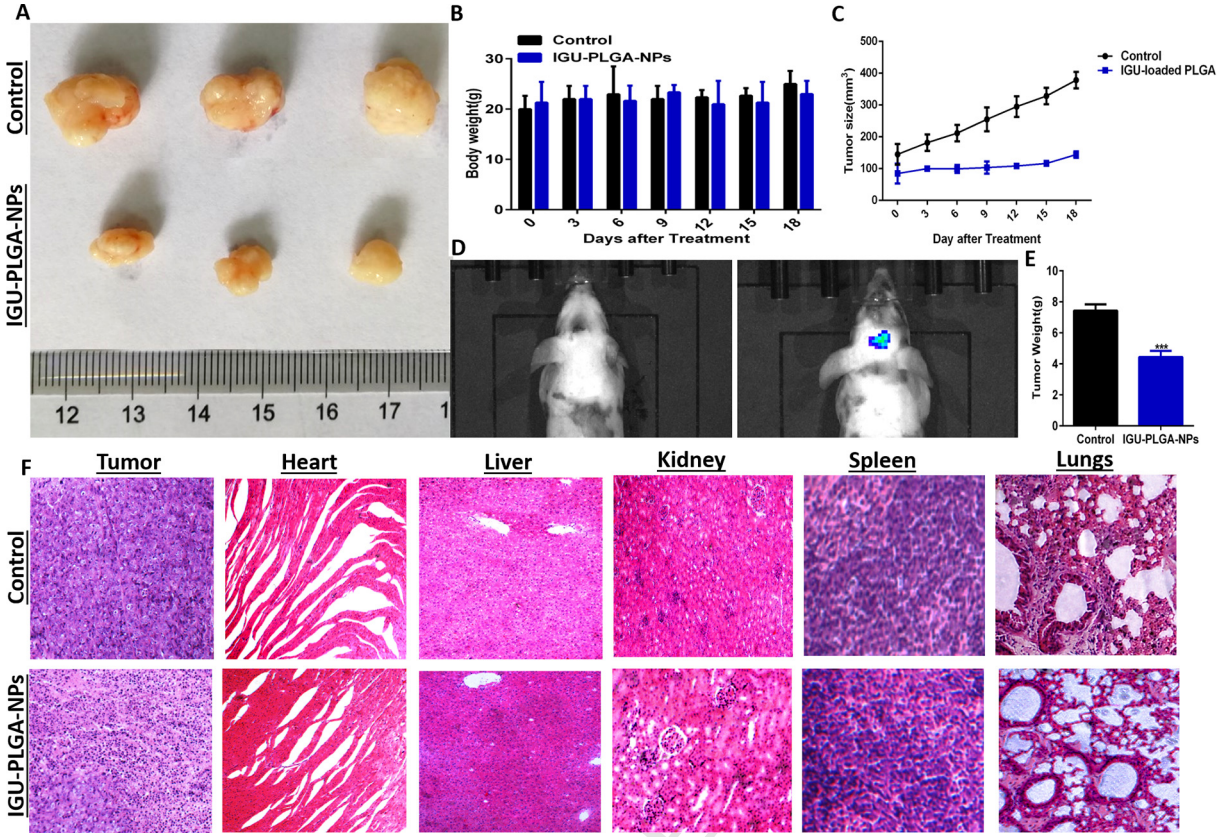

Figure 7. ***In vivo* mice xenograft model.** IGU-PLGA-NPs significantly U87 tumor growth in tumor mice model as compared to control (**A**). Graphs presenting body weight and final tumor volume and weight after administration of NPs (**B**, **C**, **E**). *In vivo* fluorescence imaging showed NPs successfully bypass BBB (**D**). Histological analysis using H&E staining of tumor and vital organs (Heart, liver, kidney, lungs and spleen) slices from NPs treated and control mice (**F**). Scale bar, 100 μm (***$P < 0.001$).

revealed the anti-cancer effect of IGU and then to maximize the therapeutic effect of IGU, we have developed IGU encapsulated-PLGA nanoparticles that are more effective therapy then IGU alone and can cross BBB, improving drug delivery and concentration at the target site. The results showed that IGU-PLGA-NPs significantly reduce the growth of glioma and glioma like stem cells. Migration of cancer cells showed a potential role in cancer metastasis.[30] The results of wound healing and Transwell assay demonstrated that IGU-PLGA-NPs treatment decreases the migration of glioma cells as compared to IGU and control.

Previous research has shown that cell cycle regulation and suppression play a vital role in cancer management.[31] The results of apoptosis and cell cycle in our study showed that the IGU-PLGA-NPs improve apoptosis and cell cycle arrest in G1 phase as compared to IGU and control. In order to explore the pathway of cell death induced in glioma cells by IGU-PLGA-NPs, we investigated the protein expression level of Bax, Bcl-2, Cytochrome c, Caspase-3 and Caspase-9 measured by western blotting. The Bcl-2 protein prevents the induction of apoptosis and blocks the release of Cytochrome c while Bax played a role in the release of Cytochrome c from the mitochondria.[32,33] We found that the Bcl-2 expression was reduced whereas Bax, Cytochrome c, Caspase-3, and Caspase-9 expression was elevated by biosynthesized IGU-PLGA-NPs. Our results indicated that NPs activates the Caspase-3, a main executioner of apoptosis and plays a significant role in apoptosis.[34]

The glioma stem cell (GSC) plays a key role in resistance of these tumors to current therapies. Our study revealed that IGU-PLGA-NPs treatment more effectively inhibits growth and tumor sphere formation of GSCs, which is also consistent with a reduction in expression of CD133 protein level in GSCs. Herein, IGU-PLGA-NPs have additional evidence for therapy strategy to overcome the chemo-resistance of TMZ on glioma cells.

In vivo, mice glioma model also showed that administration of IGU-PLGA-NPs effectively reduced the tumor growth and tumor weight, whereas uncontrolled growth was observed in control group. FL imaging presented the rapid and selective accumulation of ICG-IGU-PLGA-NPs in the brain region.

All these findings demonstrated the IGU-PLGA-NPs could inhibit tumor cell proliferation and migration, and elevate cell apoptosis and cell cycle arrest more effectively than IGU. Many factors are may be the reason for the greater anti-cancer effect of IGU-PLGA-NPs than IGU. Firstly, anti-tumor agents should have good delivery ability to cross the BBB in systemic chemotherapy against brain tumors. Secondly, IGU-PLGA-NPs

nanoparticles may release IGU continually and biodegrade gradually. Finally, interstitial chemotherapy for glioma needs a high drug concentration locally and low drug concentration in blood circulation. IGU-PLGA-NPs could enhance the efficacy of the drug and lessen systemic toxicities in glioma patients.

In conclusion, IGU-PLGA-NPs significantly inhibited proliferation and migration, decreased GSCs growth and *in vivo* tumor weight and induced apoptosis through the caspase pathway and cell cycle arrest by G1 phase in glioma cells. These results suggest that IGU-PLGA-NPs could improve malignant glioma therapy effectively. This study presents an experimental basis for clinical trials on IGU-PLGA-NPs, which may be a novel drug for therapy and management of malignant gliomas.

Appendix A. Supplementary data

Supplementary data to this article can be found online at https://doi.org/10.1016/j.nano.2019.102101.

Q7 References

1. Chen J, McKay RM, Parada LF. Malignant glioma: lessons from genomics, mouse models, and stem cells. *Cell* 2012;**149**:36-47.
2. Quail DF, Joyce JA. The microenvironmental landscape of brain tumors. *Cancer Cell* 2017;**31**:326-341.
3. Huse JT, Holland EC. Targeting brain cancer: advances in the molecular pathology of malignant glioma and medulloblastoma. *Nat Rev Cancer* 2010;**10**:319-331.
4. Cuddapah VA, Robel S, Watkins S, Sontheimer H. A neurocentric perspective on glioma invasion. *Nat Rev Neurosci* 2014;**15**:455-465.
5. Abou-Antoun TJ, Hale JS, Lathia JD, Dombrowski SM. Brain cancer stem cells in adults and children: cell biology and therapeutic implications. *Neurotherapeutics* 2017;**14**:372-384.
6. Tosi G, Bortot B, Ruozi B, et al. Potential use of polymeric nanoparticles for drug delivery across the blood–brain barrier. *Curr Med Chem* 2013;**20**:2212-2225.
7. Weaver M, Laske DW. Transferrin receptor ligand-targeted toxin conjugate (Tf-CRM107) for therapy of malignant gliomas. *J Neurooncol* 2003;**65**:3-13.
8. Pardridge WM. Drug and gene targeting to the brain with molecular Trojan horses. *Nat Rev Drug Discov* 2002;**1**:131-139.
9. Boado RJ, Pardridge WM. The Trojan horse liposome technology for nonviral gene transfer across the blood–brain barrier. *j drug deliv* 2011;**2011**:296151.
10. Lu W, Sun Q, Wan J, She Z, Jiang XG. Cationic albumin-conjugated pegylated nanoparticles allow gene delivery into brain tumors *via* intravenous administration. *Cancer Res* 2006;**66**:11878-11887.
11. Lockman PR, Oyewumi MO, Koziara JM, Roder KE, Mumper RJ, Allen DD. Brain uptake of thiamine-coated nanoparticles. *J Control Release* 2003;**93**:271-282.
12. Okamura K, Yonemoto Y, Okura C, Kobayashi T, Takagishi K. Efficacy of the clinical use of iguratimod therapy in patients with rheumatoid arthritis. *Mod Rheumatol* 2015;**25**:235-240.
13. Kohno M, Aikawa Y, Tsubouchi Y, et al. Inhibitory effect of T-614 on tumor necrosis factor-alpha induced cytokine production and nuclear factor-kappaB activation in cultured human synovial cells. *J Rheumatol* 2001;**28**:2591-2596.
14. Tu Y, Gao X, Li G, et al. MicroRNA-218 inhibits glioma invasion, migration, proliferation, and cancer stem-like cell self-renewal by targeting the polycomb group gene Bmi1. *Cancer Res* 2013;**73**:6046-6055.
15. Feng X, Zhou Q, Liu C, Tao ML. Drug screening study using glioma stem-like cells. *Mol Med Rep* 2012;**6**:1117-1120.
16. Zhang L, Wang L, Shahzad KA, et al. Paracrine release of IL-2 and anti-CTLA-4 enhances the ability of artificial polymer antigen-presenting cells to expand antigen-specific T cells and inhibit tumor growth in a mouse model. 2017; 66: 1229–41.
17. Fathima Hurmath K, Ramaswamy P, Nandakumar DN. IL-1beta microenvironment promotes proliferation, migration, and invasion of human glioma cells. *Cell Biol Int* 2014;**38**:1415-1422.
18. Hasaneen NA, Cao J, Pulkoski-Gross A, Zucker S, Foda HD. Extracellular matrix metalloproteinase inducer (EMMPRIN) promotes lung fibroblast proliferation, survival and differentiation to myofibroblasts. *Respir Res* 2016;**17**:17.
19. Hsu CY, Yi YH, Chang KP, Chang YS, Chen SJ, Chen HC. The Epstein–Barr virus-encoded microRNA MiR-BART9 promotes tumor metastasis by targeting E-cadherin in nasopharyngeal carcinoma. *PLoS Pathog* 2014;**10**e1003974.
20. National Research Council Committee for the Update of the Guide for the C and Use of Laboratory A. The National Academies Collection: reports funded by National Institutes of Health. In: th, (ed.). *Guide for the care and use of laboratory animals*. Washington (DC): National Academies Press (US) National Academy of Sciences., 2011.
21. Shahzad KA, Wan X, Zhang L, et al. On-target and direct modulation of alloreactive T cells by a nanoparticle carrying MHC alloantigen, regulatory molecules and CD47 in a murine model of alloskin transplantation. 2018; 25: 703–15.
22. Shaikh S, Rehman FU, Du T, et al. Real-time multimodal bioimaging of cancer cells and exosomes through biosynthesized iridium and iron nanoclusters. *ACS Appl Mater Interfaces* 2018;**10**:26056-26063.
23. Kim S-S, Rait A, Kim E, Pirollo KF, Chang EH. A tumor-targeting p53 nanodelivery system limits chemoresistance to temozolomide prolonging survival in a mouse model of glioblastoma multiforme. *Nanomed Nanotechnol Biol Med* 2015;**11**:301-311.
24. Oshiro S, Tsugu H, Komatsu F, et al. Efficacy of temozolomide treatment in patients with high-grade glioma. *Anticancer Res* 2009;**29**:911-917.
25. Trinh VA, Patel SP, Hwu WJ. The safety of temozolomide in the treatment of malignancies. *Expert Opin Drug Saf* 2009;**8**:493-499.
26. Yang F, Niu X, Gu X, Xu C, Wang W, Fan Y. Biodegradable magnesium-incorporated poly(l-lactic acid) microspheres for manipulation of drug release and alleviation of inflammatory response. *ACS Appl Mater Interfaces* 2019;**11**:23546-23557.
27. Higaki M, Ishihara T, Izumo N, Takatsu M, Mizushima Y. Treatment of experimental arthritis with poly(D, L-lactic/glycolic acid) nanoparticles encapsulating betamethasone sodium phosphate. *Ann Rheum Dis* 2005;**64**:1132-1136.
28. Acharya S, Sahoo SK. PLGA nanoparticles containing various anticancer agents and tumor delivery by EPR effect. *Adv Drug Deliv Rev* 2011;**63**:170-183.
29. Wong RS. Apoptosis in cancer: from pathogenesis to treatment. *J Exp Clin Cancer Res* 2011;**30**:87.
30. Wang J, Hou X, Zhao Z, Bo H, Chen Q. A cyclometalated iridium(III) complex that inhibits the migration and invasion of MDA-MB-231 cells. *Inorg Chem Commun* 2016;**67**:40-43.
31. Schwartz GK, Shah MA, Liu S, Zhu Y, Yan S, et al. Phenethyl isothiocyanate induces IPEC-J2 cells cytotoxicity and apoptosis *via* S-G2/M phase arrest and mitochondria-mediated Bax/Bcl-2 pathway. *Comp Biochem Physiol Toxicol Pharmacol* 2019:108574.
32. Li R, Ding C, Zhang J, et al. Modulation of Bax and mTOR for cancer therapeutics. *Cancer Res* 2017;**77**:3001-3012.
33. Zhang P, Wang J, Huang H, Qiao L, Ji L, Chao H. Chiral ruthenium(II) complexes with phenolic hydroxyl groups as dual poisons of topoisomerases I and IIalpha. *Dalton Trans* 2013;**42**:8907-8917.
34. MacKenzie SH, Clark AC. Targeting cell death in tumors by activating caspases. *Curr Cancer Drug Targets* 2008;**8**:98-109.

Figure S1 **Characterization of IGU-PLGA-NPs nanoparticles.** The representative graph of PLGA and IGU-PLGA-NPs size distribution (**A**, **B**) Zeta potential distribution was measured using Zeta sizer (**C**, **D**). Transmission electron microscopy micrographs of PLGA (**C**), and IGU encapsulated-PLGA nanoparticles (**D**). Scale bar: 100 nm.

Figure S2 **Trypan blue assay for cell viability.** The percentage of cell viability of U87, U118, and U251 cells was detected by trypan blue assay after IGU-PLGA NPs, IGU treatment compared with control (**A**-**C**). (***P*<0.01, ****P*<0.001 and *****P*<0.0001).

Figure S3 **Wound healing assay of glioma cells after IGU-PLGA-NPs treatment.** IGU-PLGA-NPs treated glioma cells (U87, and U118) in the wound healing assay migrated slower compared with control (**A**, **C**). The graph represents the mean ± SD rate of migration from an independent experiment performed in triplicate (**B**, **D**). (***P*<0.01, ****P*<0.001 and *****P*<0.0001).

Figure S4 **Transwell assay was conducted to determine glioma cell migration.** U87, U118, and U251 glioma cells had reduced migration ability under serum chemotaxis following culture with IGU-PLGA-NPs, compared to control cells (**A**). The graph shows the mean ± SD of migrated cells from three independent experiments (**B**-**D**). (****P*<0.001 and *****P*<0.0001).

Figure S5 **Effect of IGU-PLGA-NPs on the protein expression**. Protein expression of Bax, Bcl2, Cytochrome c, caspase3, and caspase9 was analyzed by western blotting. U87 and U251 cells were treated with IGU-PLGA-NPs and IGU as compared to control (**A**, **C**). The graph shows the relative protein expression (**B**, **D**). Data expressed as mean ± SD. (**P*<0.05, ***P*<0.01 ****P*<0.001).

Figure S6 **Effect of IGU-PLGA-NPs on the cell cycle protein expression level.** U87 and U251 cells were treated by IGU-PLGA-NPs and IGU for 24 h, then CyclinD1 and survivin protein expression was analyzed by western blotting (**A**, **C**). Relative protein expression was shown by Graph (**B**, **D**). Data expressed as mean ± SD (****P*<0.001)

Figure S7 **Blood cell count.** The treatment of IGU-PLGA NPs had no significant effect on complete blood count parameters (RBCs, WBCs, Platelets, Neutrophils, Lymphocytes, Monocytes, Basophiles and Eosinophils) when compared to control mice group (**A**-**I**) (n.s. not significant).

Figure S8 **IGU-PLGA NPs showed anti-tumor effect against U251TMZ-resistant cells.** The proliferation of U251TMZ-R cells was analyzed by CCK-8 kit assay after being treated by IGU-PLGA-NPs. IGU-PLGA-NPs significantly inhibited the proliferation of U251TMZ-R glioma cells after treatment compared to the control group (***P*<0.01).

AUTHOR QUERY FORM

ELSEVIER	**Journal: NANO** **Article Number: 102101**	**Please e-mail your responses and any corrections to:** **E-mail: Corrections.ESCH@elsevier.spitech.com**

Dear Author,

Please check your proof carefully and mark all corrections at the appropriate place in the proof (e.g., by using on-screen annotation in the PDF file) or compile them in a separate list. Note: if you opt to annotate the file with software other than Adobe Reader then please also highlight the appropriate place in the PDF file. To ensure fast publication of your paper please return your corrections within 48 hours.

For correction or revision of any artwork, please consult http://www.elsevier.com/artworkinstructions.

We were unable to process your file(s) fully electronically and have proceeded by

☐ Scanning (parts of) your article ☐ Rekeying (parts of) your article ☐ Scanning the artwork

Any queries or remarks that have arisen during the processing of your manuscript are listed below and highlighted by flags in the proof. Click on the 'Q' link to go to the location in the proof.

Location in article	**Query / Remark: click on the Q link to go** **Please insert your reply or correction at the corresponding line in the proof**
Q1	Your article is registered as a regular item and is being processed for inclusion in a regular issue of the journal. If this is NOT correct and your article belongs to a Special Issue/Collection please contact s.sudhakar@elsevier.com immediately prior to returning your corrections.
Q2	Have we correctly interpreted the following funding source(s) and country names you cited in your article: "Key Laboratory for Developmental Genes and Human Disease, Ministry of Education".
Q3	The author names have been tagged as given names and surnames (surnames are highlighted in teal color). Please confirm if they have been identified correctly.
Q4	Please provide professional degrees (e.g., PhD, MD) for the authors.
Q5, Q6	Please check unit here (millivolts [mV]?).
Q7	As per journal style, if there are more than six authors, the first six author names are listed followed by "et al."; please provide the names of the first six authors followed by "et al." for Ref (s). 6,13,14,16,21,22,24,31,32. Please check this box if you have no corrections to make to the PDF file. ☐

Thank you for your assistance.